Journal of Photochemistry and Photobiology A: Chemistry 217 (2011) 228–235

Contents lists available at ScienceDirect

Journal of Photochemistry and Photobiology A: Chemistry

journal homepage: www.elsevier.com/locate/jphotochem

Construction and photophysical properties of hypocrellin A/fullerene C_{70} supramolecular assembly

Zhize Ou[a,*], Chuanglong Guo[a], Yunyan Gao[a,*], Shayu Li[b], Weifeng Yin[a], Yi Li[c], Mimi Jin[a], Xuesong Wang[c], Guoqiang Yang[b]

[a] Department of Applied Chemistry, School of Science, Northwestern Polytechnical University, Xi'an 710072, People's Republic of China
[b] CAS Key laboratory of Photochemistry, Institute of Chemistry, Chinese Academy of Sciences, Beijing 100190, People's Republic of China
[c] Technical Institute of Physics and Chemistry, Chinese Academy of Sciences, Beijing 100190, People's Republic of China

ARTICLE INFO

Article history:
Received 14 July 2010
Received in revised form
16 September 2010
Accepted 15 October 2010
Available online 23 October 2010

Keywords:
Fullerene C_{70}
Hypocrellin
Supramolecular assembly
DNA cleavage
Photoinduced electron transfer

ABSTRACT

Interaction of hypocrellin A (HA), a naturally perylenequinonoid, with fullerene C_{70} has been studied by UV–vis and fluorescence spectra, and the results show that HA and C_{70} can form a supramolecular assembly HA/C_{70} with a 2:1 stoichiometry in organic solvents and buffer solution containing poly(vinylpyrrolidone) (PVP). The triplet lifetime of HA and C70 are reduced due to the formation of supramolecular complex. Electron paramagnetic resonance (EPR) studies suggest that photoinduced electron transfer from N,N,N′N′-tetramethyldiethyleneamine (TMEDA) to the excited HA induces the generation of anion radical of HA ($HA^{\bullet-}$), followed by further electron transfer from $HA^{\bullet-}$ to C_{70}. HA can mediate the electron transfer from TMEDA to C_{70} and significantly enhance the intensity of characteristic Near-IR absorption transition of $C_{70}^{\bullet-}$, through efficient electron-transfer processes. Upon visible light irradiation, HA/C_{70} exhibits stronger photodamage ability on calf thymus DNA under anaerobic condition than HA and C_{70}.

1. Introduction

Recently, supramolecular architectures, especially employing fullerenes as 3-dimensional building blocks, have received considerable attention for their potential applications in medical fields, nanoscale photonic devices and sensors [1–4]. Inclusion of fullerenes with π-extended molecules, including porphyrin, perylene, tetrathiafulvalene and phthalocyanine [5–14], via π-electronic interactions is highly interesting, which can provide the possibility of modulating the electronic properties of fullerenes. The design of supramolecular recognition elements of fullerene, revealing complex energy- and/or electron-transfer processes, is important for the development of supramolecular chemistry of fullerene [15–17].

Fullerenes possess small reorganization energy in electron transfer, which leads to remarkable acceleration of charge separation and deceleration of charge recombination [18,19]. The covalently conjugated fullerene C_{60}-quinone organofulerenes have been reported to be excellent electron-accepting system [20–23]. Recently, the quinones with large aromatic rings, such as anthraquinones, have been employed to construct noncovalent supramolecular complex with fullerene C_{60} [24–26]. These anthraquinones can mediate photoinduced electron transfer from electron donors to fullerenes and generate long-lived charge-separated state.

Hypocrellins, a type of naturally occurring perylenequinonoid, exhibit efficient photodynamic activity against a large variety of tumor cell lines and viruses [27,28]. The maganesium complex of hypocrellin A (Mg^{2+}–HA) can form a supramolecular assembly with C_{60}, and improve the solubility of C_{60} significantly [29,30]. The resulting supramolecular assembly exhibits much stronger DNA-damaging ability than Mg^{2+}–HA due to the introduction of C_{60} as a final electron acccptor. Fullerene C_{70} possesses higher DNA photocleavage efficiency upon irradiation than C_{60} [31]. However, to the best of our knowledge, the interaction between hypocrellins and fullerenes other than C_{60} has not been reported.

In this work, the interaction between HA and fullerene C_{70} is investigated. The energy- and electron-transfer processes in HA/C_{70} system are studied in detail. HA/C_{70} complex shows much more efficient photocleavage ability towards DNA under anaerobic condition than free HA and C_{70}, which suggests that the fullerene-based supramolecular systems can be explored for biomedical application in general and in particular for photodynamic therapy [32,33].

* Corresponding authors. Tel.: +86 29 88431677; fax: +86 29 88431677.
E-mail addresses: ouzhize@nwpu.edu.cn (Z. Ou), gaoyunyan@nwpu.edu.cn (Y. Gao).

1010-6030/$ – see front matter © 2010 Elsevier B.V. All rights reserved.
doi:10.1016/j.jphotochem.2010.10.014

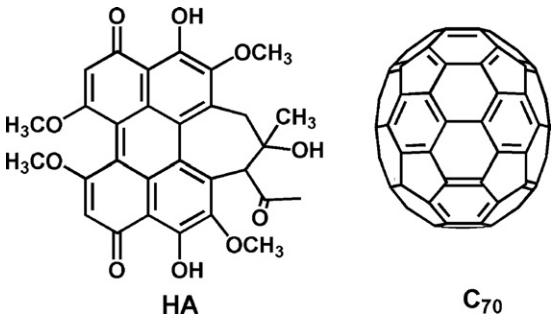

Fig. 1. The chemical structure of HA and C_{70}.

2. Experimental

2.1. Chemicals

HA was isolated from the fungus sacs of hypocrella bambusae and recrystallized twice from acetone before use (Fig. 1) [34]. Calf thymus DNA (CT DNA), Ethidium bromide (EB), fullerene C_{70}, N,N,N′,N′-tetramethylethylenediamine (TMEDA) and poly(vinylpyrrolidone) (PVP) were purchased from Sigma Chemical Company, without further processing before use. The aqueous solutions of HA and C_{70} were prepared with PVP as reported previously, and used for DNA cleavage experiments [35]. All the solvents were purchased from Beijing Chemical Factory and distilled before use.

2.2. Measurements of spectral and electrochemical properties

Steady state absorption and fluorescence spectra were recorded with a Hitachi UV-3010 UV–vis spectrophotometer, PerkinElmer Lambd 950 UV/vis/NIR spectrophotometer and Hitachi F-4600 spectrofluorimeter, respectively. The fluorescence experiments were carried out in a 5 mm × 5 mm cuvette and HA was selectively excited at 470 nm.

Fluorescence quantum yield (Φ_F) of HA was determined with rhodamine 6G (Φ_R = 0.97, methanol) [36] as a reference in Eq. (1):

$$\frac{\Phi_S}{\Phi_R} = \frac{A_S}{A_R} \times \frac{OD_R}{OD_S} \times \frac{n_S^2}{n_R^2} \quad (1)$$

where S and R stand for sample and the reference, respectively. Φ, *A*, OD and *n* stand for the fluorescence quantum yield, the fluorescence spectral areas from 550 nm to 750 nm, the optical densities at the excitation wavelength and the refractive index of the solvents, respectively.

Fluorescence lifetimes were measured by time-correlated single-photon counting technique with Edinburgh FL-900 spectrophotometer upon 400 nm laser pulse irradiation.

Nanosecond transient absorption spectra were performed on a LP-920 pump-probe spectroscopic setup (Edinburgh). The excited source was the unfocused second harmonic (532 nm) output of a Nd:YAG laser (Continuum surelite II); the probe light source was a pulse-xenon lamp. The signals were detected by Edinburgh analytical instruments (LP900) and recorded on a Tektronix TDS 3012B oscilloscope and a computer [37]. A liquid-nitrogen-cooled germanium (Ge) detector was used to monitor the emission signal in the NIR spectral range [38].

EPR spectra were obtained using a Bruker ESP-300E spectrometer operating at room temperature. Samples were injected into the specially made quartz capillaries for analysis, purged with argon for 30 min in the dark, and illuminated directly in the cavity of the spectrometer with a Nd:YAG laser (532 nm).

Cyclic voltammetry (CV) experiments were performed on a CHI660C electrochemical workstation by a cyclic voltammetry (CV) technique in DMSO–toluene (4/1, v/v) solution, using two platinum wires as the working and counter electrodes, respectively, and a saturated calomel electrode (SCE) as reference electrode in the presence of 1 mM n-tetrabutylammonium perchlorate as the supporting electrolyte [39].

2.3. Fluorescence Job's plot of HA with C_{70}

Stock solutions of HA (50 μM) and C_{70} (50 μM) were prepared, and the solutions with molar fraction of HA from 0.1 to 0.9 were prepared in 5 ml volumetric flasks by diluting the required amount of the stock solutions. The total concentration of HA and C_{70} was fixed at 50 μM. The difference of fluorescence intensity (ΔF) could be calculated according to the following equation (Eq. (2)):

$$\Delta F = F_{mix} - F_{HA} - F_{C_{70}} \quad (2)$$

where F_{mix}, F_{HA} and $F_{C_{70}}$ were the fluorescence of the mixed solution, free HA and free C_{70} at corresponding concentration, respectively.

2.4. Fluorescence titration

The titrations were performed by adding the required volumes of a solution of C_{70} (1 mM) into the solution of HA (10 μM). The association constants of the HA/C_{70} complex were determined by Benesi–Hildebrand method in a variety of solvents [40].

Under experimental conditions, the fluorescence of HA decreased with increasing C_{70} concentration (Eq. (3)).

$$\begin{array}{ccc} HA + 0.5C_{70} & \xrightarrow{K_a} & HA/(C_{70})_{0.5} \\ (1-a)[HA] & [C_{70}] - 0.5a[HA] & a[HA] \end{array} \quad (3)$$

where *a* was the degree of association between HA and C_{70}, K_a is the binding constant. K_a could be calculated according to Eq. (4):

$$K_a = \frac{a[HA]}{(1-a)[HA] \times ([C_{70}] - 0.5a[HA])^{1/2}} \quad (4)$$

At relative high concentration of $[C_{70}] \gg [HA]$, *a* was given by Eq. (5):

$$a = \frac{K_a[C_{70}]^{1/2}}{1 + K_a[C_{70}]^{1/2}} \quad (5)$$

The observed fluorescence (*F*) of HA could be related to the fluorescence of uncomplexed (F_0) and complexed (F') molecules of HA by the following equation:

$$F = (1-a)F_0 + aF' \quad (6)$$

Eq. (6) could be simplified to the form (Eq. (7)):

$$F_0 - F = a(F_0 + F') \quad (7)$$

From Eqs. (5) and (7), the following relation (Eq. (8)) could be obtained. A double reciprocal plot could be made with $1/(F_0 - F)$ as a function of $[C_{70}]^{-1/2}$, and the K_a could be calculated from the slope.

$$\frac{1}{F_0 - F} = \frac{1}{F_0 - F'} + \frac{1}{K_a(F_0 - F')[C_{70}]^{1/2}} \quad (8)$$

2.5. Examination of DNA-cleavage ability

A simple assay for DNA cleavage was applied based on ca. 20-fold enhancement of the fluorescence intensity exhibited by EB upon intercalation into DNA [41,42]. When the concentration of EB was two-fold higher than that of the DNA base pair, the fluorescence

intensity of EB was linearly proportional to the concentration of the DNA base pair. Any process in which the potential EB binding site was destroyed results in a decrease in fluorescence intensity.

To a 10 mL EB/DNA buffer solution (80 μM EB, 40 μM DNA) was added the concentrated photosensitizers. The final concentration of PVP was fixed at 0.05%. Then the solution was divided into 4 aliquots, purged with argon for 15 min, and irradiated in a "merry-go-round" apparatus with a medium pressure sodium lamp ($h\nu > 470$ nm). The aliquots were removed at various time t and their fluorescence emissions in the range of 525–700 nm were measured by exciting at 510 nm.

The percentage of binding site remaining (BSR%) at a given time was calculated from Eq. (9):

$$\text{BSR\%} = 100 \times 1 - \left(\frac{I_0 - I_t}{I_0 - I_{\text{buffer}}}\right) \quad (9)$$

where I_0, I_t, I_{buffer} denoted the integrated fluorescence intensities before irradiation, after t min of irradiation, and of DNA-free buffer, respectively.

3. Results and discussions

3.1. Absorption spectra

As shown in Fig. 2, both HA and C_{70} (Fig. 2a, inset) have strong absorption in the visible region. HA exhibits three absorption peaks at 468, 542, and 584 nm, while C_{70} displays four absorption peaks at 330, 359, 377, 468, and 636 nm, respectively [43,44]. The interaction between HA and C_{70} in toluene is studied by titration experiments. In detail, the toluene solution of HA was titrated with variable amounts of C_{70} and the changes were routinely monitored by absorption spectra (Fig. 2a).

Continuous changes were observed in the UV–vis differential absorption spectra upon addition of C_{70} to the HA solution (Fig. 2b). Usually, the differential absorption spectra could changes with not only positive but also negative in intensity for the strong interaction exists [29]. However, the differential absorption spectra in Fig. 2b are similar to that of C_{70} in term of the shape, which suggest that HA bound to C_{70} with moderate interaction. Similar observations have been reported for the complexation of fullerene with cyclotriveratrylene derivatives [45,46]. Indeed, these results are indications of fullerene complexation, as previously reported for fullerene containing supramolecular adducts [47,48].

3.2. Fluorescence spectra

HA possesses moderate fluorescence quantum yields in organic solvents and buffer solution (Table 1). The interaction between HA and C_{70} is further investigated using steady-state fluorescence measurement. Upon addition of C_{70}, the fluorescence intensity of HA decreases gradually (Fig. 3). The dependence of the fluorescence intensity of HA on the concentration of C_{70} follows Stern–Volmer equation (Eq. (10)) [39], in which F_0 and F are the fluorescence intensity of HA in the absence and presence of quencher C_{70}, respectively. K_q is the quenching rate constant, τ_0 is the average

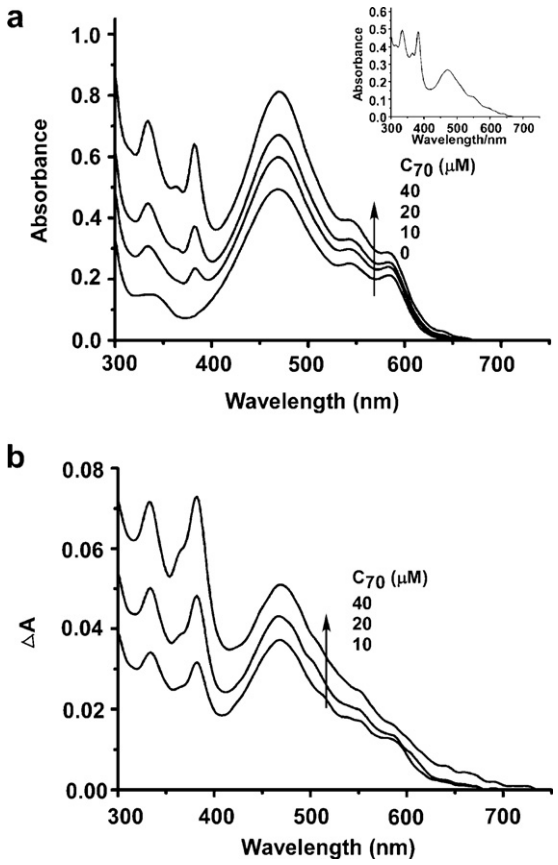

Fig. 2. (a) Absorption and (b) differential absorption spectral changes of HA (80 μM) upon titration with C_{70} in toluene. (Inset) Absorption spectrum of C_{70} (40 μM) in toluene.

fluorescence lifetime of HA in the absence of C_{70}, which was determined by time-correlated single-photon counting technique [49].

$$\frac{F_0}{F} = 1 + K_q \tau_0 [C_{70}] \quad (10)$$

The representive Stern–Volmer plot of HA quenching monitored at 608 nm is constructed as shown in Fig. 3 inset. The K_q values in solvents ($1.24–2.45 \times 10^{13}$ L mol^{-1} s^{-1}) calculated from Stern–Volmer plots (Table 1) are much higher than that of the diffusion rate constant (10^{10} L mol^{-1} s^{-1}), indicating that some type of interaction between HA and C_{70} exists. To verify the possibility of dynamic quenching, fluorescence lifetime measurements are carried out. The fluorescence lifetime of HA (τ_0) was determined to be around 1.05 ns in toluene in the absence of quencher C_{70} (Fig. 3b) [49]. There is almost no change in lifetime of HA after addition of C_{70} (1.03 ns). These results suggest that C_{70} quenches fluorescence of HA through static quenching mechanism, due to the formation of nonfluorescent ground state complex between C_{70} and HA.

Fluorescence Job's plots are constructed to determine the stoichiometry of HA/C_{70} complex by monitoring the fluorescence at 608 nm [50]. The Job's plots reveal breaks around 0.32 for the molar

Table 1
Stern–Volmer quenching constants (K_q) and binding constants (K_a) for the interaction of HA with C_{70} in different media.

Solvent	Φ_F[a]	τ_0 (ns)	$K_q \times 10^{-13}$ (L mol^{-1} s^{-1})	K_a (M$^{-1/2}$)
Toluene	0.15	1.05	2.45 (R = 0.99675)	136.9 (R = 0.9986)
Anisole	0.13	1.12	2.13 (R = 0.9961)	116.5 (R = 0.9948)
Toluene-DMSO	0.15	1.33	1.43 (R = 0.9973)	68.5 (R = 0.9988)
1% PVP[b]	0.09	0.75	1.24 (R = 0.9941)	64.6 (R = 0.9952)

[a] Φ_F: fluorescence quantum yield of HA with rhodamine 6G as the reference.
[b] In 10 mM Tris–HCl buffer solution (pH 7.0).

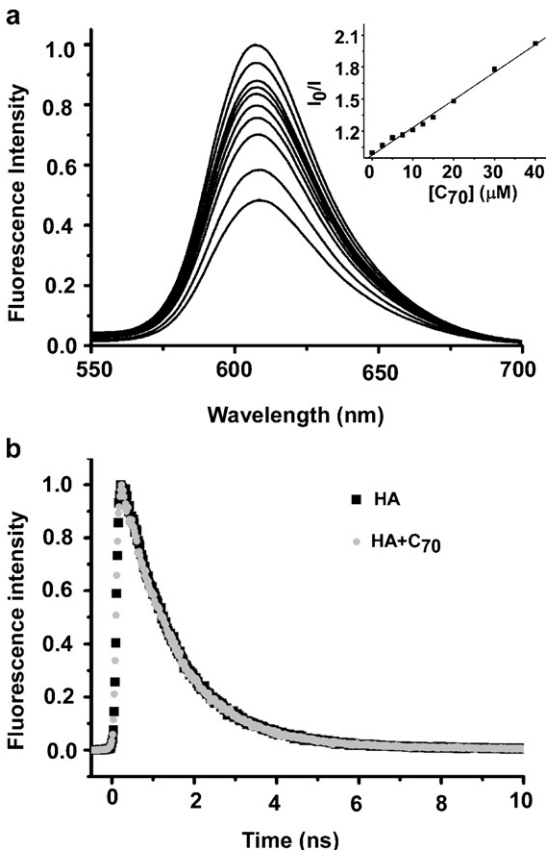

Fig. 3. (a) Fluorescence emission spectra changes upon addition of C_{70} to a solution of HA (10 μM) in toluene (λ_{ex} = 470 nm). [C_{70}] = 0, 2.5, 5, 7.5, 10, 12.5, 15, 20, 30, 40 μM. (b) Fluorescence decay of HA (10 μM) at 608 nm in the absence (black) and presence (gray) of C_{70} (40 μM) in toluene (λ_{ex} = 410 nm). (Inset) Stern–Volmer plot for the fluorescence quenching of HA at 608 nm by C_{70} in toluene solution.

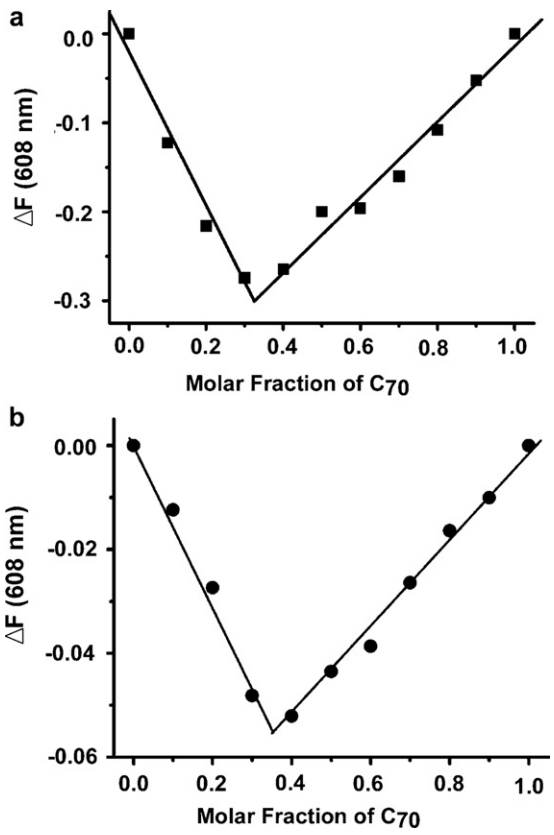

Fig. 4. Job's plot for the complexation of HA with C_{70} in (a) toluene and (b) 1% PVP buffer solution. [HA] + [C_{70}] = 50 μM (λ_{ex} = 470 nm).

fraction of C_{70}, suggesting a 2:1 molar ratio of HA and C_{70} in the complex (Fig. 4).

The binding constants K_a are evaluated by the Benesi–Hildebrand method using the fluorescence spectral changes (Fig. 5). The good linear relationship with $R \geq 0.9930$ in Benesi–Hildebrand plots supported the 2:1 binding model for HA/C_{70} supramolecular assembly in different solvents (Table 1). The quenching rate constant K_q and binding constant K_a are generally lower in polar solvents, which can be attributed to the limited solubility and subsequent aggregation of C_{70} in toluene-DMSO (v/v, 4/1) and 1% PVP buffer solution [51–53].

As it appears from the formulate, HA shares an axial chirality with many other natural perylenequinones due to the steric hindrance of the methoxy groups in the "left" moiety and of the seven-membered ring in the "right" moiety, which leads to the twist conformation of HA [54,55]. The axial chirality of HA may facilitate its interaction with fullerenes through the concave surface [56–58].

Our previous results demonstrated that HA cannot form stable complex with fullerene C_{60} [29,30]. The increased binding affinity in HA/C_{70} complex can be attributed to the ovoid shape of C_{70} which allows better contact between the C_{70} surface and HA units. It has been reported that porphyrin hosts tend to prefer larger fullerenes due to the greater π–π contact area between their π-electronic surface [14,59]. The nature of the binding of HA to C_{70} may be due to the π–π stacking interactions, as in the case of noncovalent binding of aromatic component with fullerenes [5–14]. The formaiton of HA/C_{70} supramolecular assembly with 2:1 ratio, but not 1:1, which can be atrributed to the more stable π–π stacking interaction in the complex of 2:1 stoichiometry as that in Mg^{2+}–HA/C_{60} [29]. Collectively, these observations suggest that the chiral conformation of HA and the preferred π–π stacking interaction are very important for the construction of HA/C_{70} complex.

3.3. Transient absorption spectra

Information on the dynamic excited-state interactions in HA/C_{70} is obtained by utilizing transient absorption spectra in the visible regions. HA presents characteristic triplet absorption bands with maxima around 390, 530, 570 and 610 nm, and for C_{70}, the triplet absorption bands appear at 400 and 580 nm [60,61]. HA/C_{70} com-

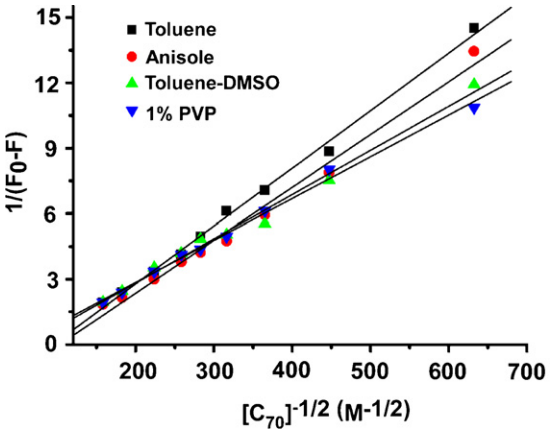

Fig. 5. Benesi–Hildebrand plot constructed to evaluate the binding constant of HA with C_{70}, based on the 2:1 binding model.

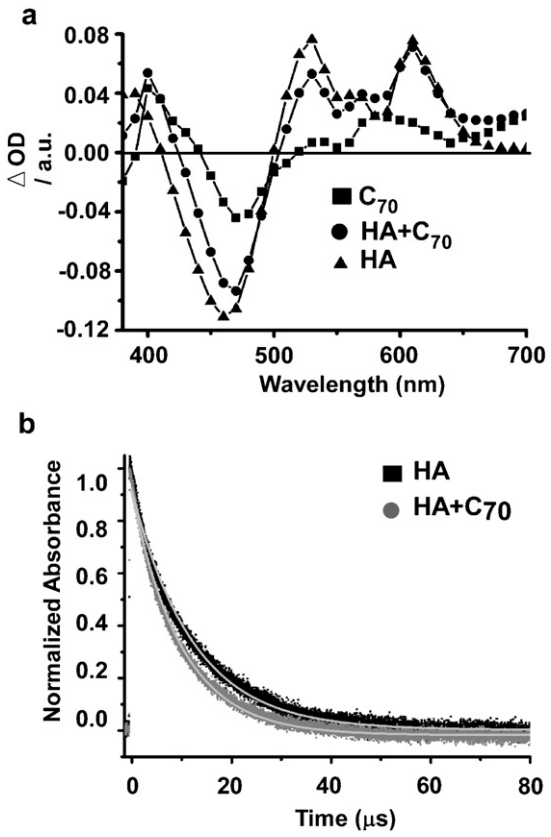

Fig. 6. (a) Transient difference absorption spectra from a solution of HA (40 μM), C_{70} (20 μM) and the mixed solution of HA (40 μM) and C_{70} (20 μM). (b) Time profile of the transient absorption bands of the HA at 530 nm in the absence and presence of C_{70}.

plex displays almost all the characteristic peaks for triplet HA and C_{70} (Fig. 6a).

Fig. 6b shows the decay traces of HA and HA/C_{70}, taking the transient spectra of HA and HA/C_{70} at 530 nm as a function of time. The decay curve for HA can be fitted monoexponentially with lifetime of 12.6 μs. While the decay curve for HA/C_{70} system can be fitted double-exponentially with lifetimes of 11.5 μs (A_1 = 77%) and 3.12 μs (A_2 = 23%). The longer lifetime component can be assigned to the triplet state of pristine HA and the shorter time component may be because of the interaction between triplet HA and C_{70}.

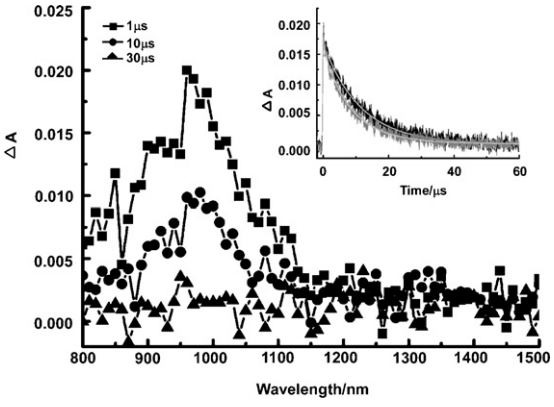

Fig. 7. Transient absorption spectra observed by 532 nm laser irradiation of C_{70} (50 μM) at 1 (■), 10 (●), 30 μs(▲) in Ar-saturated DMSO-toluene (4/1, v/v). (Inset) Absorption time profiles of C_{70} at 980 nm in the absence (black line) and presence of HA (100 μM) (gray line).

Further studies involving the nanosecond transient absorption spectra of C_{70} in NIR region are also performed (Fig. 7). The triplet decay of $^3C_{70}$ at 980 nm obeys first-order kinetics with τ = 12.0 μs [62–64]. In the presence of HA, the triplet decay of C_{70} trace could be fitted to a biexponential decay with lifetimes of 11.8 (A_1 = 60%) and 5.96 (A_2 = 40%) μs (Fig. 7, inset). Collectively, the transient absorption studies indicate that the triplet lifetimes of HA and C_{70} are reduced after formation of HA/C_{70} complex.

One may argue that electron transfer might occur in HA/C_{70} system, considering that fullerenes are excellent electron acceptors [65]. Free energy change (ΔG) involving electron transfer from the excited state of HA to the ground state of C_{70} is a thermodynamically unfavorable process (ΔG = 0.07 eV), calculated by Rehm–Weller equation (Eq. (11)), using oxidation potential of HA (1.47 V vs SCE), first reduction potential of C_{70} (−0.44 V vs SCE), and triplet state energy of 1.84 eV for HA [61]. Furthermore, the transient absorption attributable to the anion radical C_{70} cannot be detected. As a result, the electron transfer between excited state of HA and C_{70} can be ruled out.

$$\Delta G = E_{ox}\ (\text{donor}) - E_{red}\ (\text{receptor}) - E^*\ (\text{donor or acceptor}) \quad (11)$$

On the other hand, the triplet energy of C_{70} (35.0 kcal mol^{-1}) [66] is lower than that of HA (42.5 kcal mol^{-1}) [61]. Direct triplet–triplet energy transfer from the triplet excited HA to C_{70} is thermodynamically possible. However, decay of the triplet HA at 530 nm and the rise of triplet C_{70} at 980 nm do not simultaneously occur. As a result, the triplet–triplet energy transfer between HA and C_{70} is not efficient, and may not be the main reason for the reduced triplet lifetime of HA and C_{70} after formation of HA/C_{70} complex. Taking insight into the structure of HA, which possesses large aromatic rings, the nature of the binding of C_{70} to HA may be attributed to π–π stacking interaction between perylenequinonoid ring of HA and the cage of C_{70}. In closely packed fullerene clusters, the triplet lifetime of fullerene and photosensitizers is very sensitive to the environment and reduced due to the formation of supramolecular complexes [67,68].

3.4. EPR spectra studies

EPR, as a powerful technique for investigating photoreaction intermediates, is employed to study the mechanism of electron transfer in HA/C_{70} complex in the presence of electron donor TMEDA. After irradiation of the mixture of HA and TMEDA in the argon-saturated DMSO-toluene solution for 2 min, an EPR signal can be observed (Fig. 8a). The g value (2.002) of this signal correlates well with that of HA semiquinone anion radical ($HA^{\bullet-}$) [69]. The generation of $HA^{\bullet-}$ can originate from the photoinduced electron transfer from TMEDA to excited HA (Eq. (12)):

$$HA^* + TMEDA \rightarrow HA^{\bullet-} + TMEDA^{\bullet+} \quad (12)$$

Upon addition of deoxygenated solution of C_{70} to the above irradiated solution, the EPR signal of $HA^{\bullet-}$ is remarkably quenched and a new EPR signal (g = 2.003) appears simultaneously (Fig. 8b). Control experiment indicates that the EPR signal of C_{70} anion radical ($C_{70}^{\bullet-}$), generated from photoinduced electron transfer from TMEDA to excited C_{70} (Eq. (13)), has same g value and position as that of the new signal (Fig. 8c) [70]. The first reduction potential of C_{70} (−0.44 V vs SCE) is more positive than that of HA (−0.56 V vs SCE), which suggests electron transfer from $HA^{\bullet-}$ to C_{70} is a thermodynamically favorable process (Eq. (14)) (ΔG = −0.127 eV), calculated from Eq. (15). These EPR results suggest that HA can medicate the electron transfer from reductant TMEDA to the

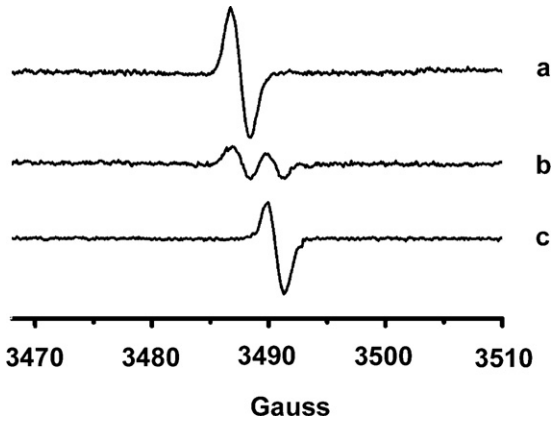

Fig. 8. (a) Photoinduced EPR spectrum of deoxygenated solution of TMEDA (1 mM) and HA (120 μM) in DMSO-toluene (4/1, v/v) upon irradiation at 532 nm for 2 min. (b) Similar to (a), but with the addition of C_{70} (60 μM) after irradiation. (c) Similar to (a), but C_{70} (60 μM) instead of HA.

ground state C_{70}.

$$C_{70}^{*} + \text{TMEDA} \rightarrow C_{70}^{\bullet -} + \text{TMEDA}^{\bullet +} \quad (13)$$

$$C_{70} + \text{HA}^{\bullet -} \rightarrow C_{70}^{\bullet -} + \text{HA} \quad (14)$$

$$\Delta G = E_{\text{red}} \ (\text{donor}) - E_{\text{red}} \ (\text{acceptor}) \quad (15)$$

3.5. NIR absorption spectra

Upon irradiation of the solution of HA/C_{70} in the presence of TMEDA with medium pressure sodium lamp for 5 min, a NIR absorption band at 1368 nm is observed, which is the characteristic NIR absorption transition of $C_{70}^{\bullet -}$ (Fig. 9a) [71,72]. In the absence of HA, the intensity of the NIR absorption band of $C_{70}^{\bullet -}$ decreases about 35% (Fig. 9b). Control experiments confirm that C_{70} and light are all essential for the NIR absorption band generation of $C_{70}^{\bullet -}$ (Fig. 9c).

According to our above experimental results, in principle, two different processes can be accounted for the generation of $C_{70}^{\bullet -}$ in HA/C_{70}/TMEDA system. (1) $C_{70}^{\bullet -}$ can be generated from direct electron transfer from the reductant TMEDA to the excited stated C_{70} (Eq. (13)). (2) one-electron transfer from TMEDA to excited-state HA induces the generation of $HA^{\bullet -}$, followed by electron transfer from $HA^{\bullet -}$ to C_{70}, forming the corresponding anion radical $C_{70}^{\bullet -}$(Eqs. (12) and (14)). As a result, the NIR absorption intensity of $C_{70}^{\bullet -}$ for HA/C_{70} in the presence of TMEDA is much higher than

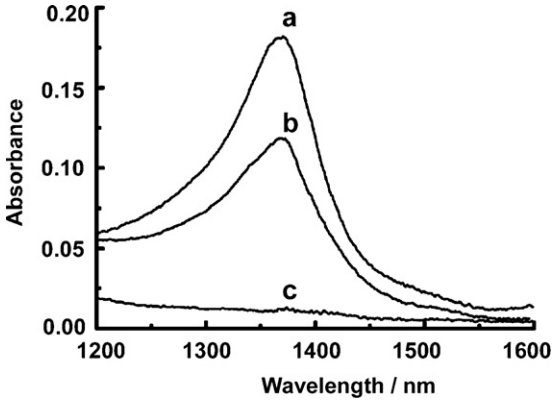

Fig. 9. (a) NIR absorption spectra for argon-saturated DMSO-toluene (4/1, v/v) solution of HA (120 μM), C_{70} (60 μM), and TMEDA (1 mM) upon illuminated with medium pressure sodium lamp for 5 min. (b) Similar to (a) but in the absence of HA. (c) Similar to (a) but C_{70} or light is omitted.

Table 2
Photodamage of CT DNA by HA, C_{70} and HA/C_{70} detected by the remaining binding site (BSR%) of ethidium bromide to the damaged CT DNA under anaerobic condition[a] ([CT DNA] = 40 μM, [EB] = 80 μM).

Samples	BSR% at varied irradiation		
	5 min	10 min	15 min
Control experiment[b]	99.1	98.5	98.0
HA[c]	95.6	85.8	79.0
C_{70}[d]	96.2	92.2	89.5
HA/C_{70}[e]	86.5	71.2	64.1
Mg^{2+}–HA/C_{60}[f]	93.8	81.5	72.2

[a] Each point represents the mean of three separate experiments.
[b] Without photosensitizer.
[c] [HA] = 8 μM.
[d] [C_{70}] = 4 μM.
[e] [HA] = 8 μM, [C_{70}] = 4 μM.
[f] [Mg^{2+}–HA] = 8 μM, [C_{60}] = 4 μM.

that for C_{70} in the presence of TMEDA upon irradiation, due to the efficient electron-transfer processes in HA/C_{70}.

3.6. Photoinduced damage of DNA

Hypoxia is a common feature of both human and animal tumors [73,74]. Enhancement of the photodynamic efficacy under hypoxic condition is one possible way to improve the therapeutic capability of photosensitizers. HA and C_{70} can form a supramolecular system in PVP buffer solution (Figs. 4b and 5), which may facilitate studies of biological properties of HA/C_{70} complex.

Photosensitized damage of CT DNA by HA, C_{70} and HA/C_{70} complex is characterized by the simple EB assay, and the remaining binding site percentages after varied irradiation time are collected in Table 2. Upon visible light irradiation, the binding sites of CT DNA destroyed by HA/C_{70} are more than the sum of those by HA and C_{70} under anaerobic condition. For example, upon irradiation for 5 min, the binding sites of CT DNA destroyed by HA, C_{70}, and HA/C_{70} are 4.4, 3.8, 14.5%, respectively. Under anaerobic conditions, the photodamage of CT DNA by HA, C_{70} and HA/C_{70} complex is presumably due to electron transfer from DNA to the excited-state HA or C_{70} [75,76]. For the HA/C_{70} system, electron transfer first from DNA to the excited-state HA (Eq. (16)) may occur and then further from $HA^{\bullet -}$ to C_{70} (Eq. (14)), and photoinduced electron transfer from DNA to excited-state C_{70} may also take place (Eq. (17)).

$$\text{HA} + \text{DNA} \rightarrow \text{HA}^{\bullet -} + \text{DNA}^{\bullet +} \quad (16)$$

$$C_{70} + \text{DNA} \rightarrow C_{70}^{\bullet -} + \text{DNA}^{\bullet +} \quad (17)$$

It has been reported that suppression of the back electron transfer is very important for enhancement of the DNA photodamage capability of photosensitizers [77]. Fullerenes, as excellent electron acceptors, possess smaller reorganization energy in electron transfer processes, which can leads to significant acceleration of charge separation and effective deceleration of charge recombination [18,19]. The HA/C_{70} supramolecular assembly is organized as an electron acceptor system, following an electrochemical gradient, which can promote a unidirectional electron transfer cascade (Eq. (12) and Eq. (14)) [78,79]. As a result, HA/C_{70} presents much stronger photocleavage ability on DNA than HA and C_{70} under anaerobic conditions.

Our previous studies demonstrate that Mg^{2+}–HA can act as light-harvesting in the Mg^{2+}–HA/C_{60} supramolecular system and mediate the electron transfer reaction between DNA and C_{60} [29]. It is interesting to compare the DNA photodamage capability of Mg^{2+}–HA/C_{60} and HA/C_{70}. Although HA displays weaker DNA damage capability than Mg^{2+}–HA [29], HA/C_{70} cause stronger DNA cleavage than Mg^{2+}–HA/C_{60} under anaerobatic condition (Table 2). The enhanced DNA damage capability of HA/C_{70}, com-

pared with Mg^{2+}–HA/C_{60}, can be attributed to the difference of the type of fullerene in these supramolecular systems. It has been reported that fullerene C_{60} and C_{70} exhibit similar electrochemical properties [39], however, C_{70} can cause stronger DNA damage than C_{60} because of its stronger absorption in visible region [31]. Fullerenes act as final electron acceptors in these hypocrellin/fullerene supramolecular assemblies and significantly promote DNA damage capability of hypocrellins.

4. Conclusion

In summary, a supramolecular system consisting of HA and C_{70} has been constructed and characterized. HA acts as light harvesting antenna in supramolecular system and promote the photoinduced electron transfer between C_{70} and reductants (TMEDA, DNA, etc.), through efficient electron-transfer processes. HA/C_{70} present stronger DNA damage capability than Mg^{2+}–HA/C_{60} complex, due to the strong absorption of C_{70} in visible region.

Acknowledgments

This research is supported by SRF for ROCS, SEM (N9YK0003, N9YK0005), NPU Foundation for Fundamental Research (NPU-FFR-W018113), and Ao Xiang Foundation for Youth NPU teachers (07XE0152), which are gratefully acknowledged.

References

[1] E.M. Perez, B.M. Illescase, M.A. Herranz, N. Martin, Supramolecular chemistry of π-extended analogues of TTF and carbon nanostructures, New J. Chem. 33 (2009) 228–234.
[2] R. Chitta, F. D'Souza, Self-assembled tetrapyrrole–fullerene and tetrapyrrole–carbon nanotube donor–acceptor hybrids for light induced electron transfer applications, J. Mater. Chem. 18 (2008) 1440–1471.
[3] D.M. Guldi, G. Rahman, V. Sgobba, C. Ehli, Multifunctional molecular carbon materials-from fullerenes to carbon nanotubes, Chem. Soc. Rev. 35 (2006) 471–487.
[4] E. Nakamura, H. Isobe, Functionalized fullerenes in water. The first 10 years of their chemistry, biology, and nanoscience, Acc. Chem. Res. 36 (2003) 807–815.
[5] Y. Eda, K. Itoh, Y.N. Ito, T. Kawato, 2,6-Bis(porphyrin)-substituted pyrazine: a new class of supramolecular synthon binding to a transition-metal ion and fullerene (C_{60}), Tetrahedron 65 (2009) 282–288.
[6] F. D'Souza, O. Ito, Supramolecular donor–acceptor hybrids of porphyrins/phthalocyanines with fullerenes/carbon nanotubes: electron transfer, sensing, switching, and catalytic applications, Chem. Commun. (2009) 4913–4928.
[7] S. Fukuzumi, T. Kojima, Photofunctional nanomaterials composed of multiporphyrins and carbon-based p-electron acceptors, J. Mater. Chem. 18 (2008) 1427–1439.
[8] K. Tashiro, T. Aida, Metalloporphyrin hosts for supramolecular chemistry of fullerenes, Chem. Soc. Rev. 36 (2007) 189–197.
[9] D. Canevet, M. Salle, G. Zhang, D. Zhang, D. Zhu, Tetrathiafulvalene (TTF) derivatives: key building-blocks for switchable processes, Chem. Commun. (2009) 245–2256.
[10] R. Bhosale, J. Miek, N. Sakai, S. Matile, Supramolecular n/p-heterojunction photosystems with oriented multicolored antiparallel redox gradients, Chem. Soc. Rev. 39 (2010) 138–149.
[11] G. Bottari, D. Olea, C. Gomez-Navarro, F. Zamora, J. Gomez-Herrerro, T. Torres, Highly conductive supramolecular nanostructures of a covalently linked phthalocyanine–C_{60} fullerene conjugate, Angew. Chem. Int. Ed. 47 (2008) 2026–2031.
[12] F. D'Souza, E. Maligaspe, K. Ohkubo, M.E. Zandler, N.K. Subbaiyan, S. Fukuzumi, Photosynthetic reaction center mimicry: low reorganization energy driven charge stabilization in self-assembled cofacial zinc phthalocyanine dimer-fullerene conjugate, J. Am. Chem. Soc. 131 (2009) 8787–8797.
[13] H. Imahori, T. Umeyama, Donor-acceptor nanoarchitecture on semiconducting electrodes for solar energy conversion, J. Phys. Chem. C 113 (2009) 9029–9039.
[14] P.D.W. Boyd, C.A. Reed, Fullerene-porphyrin constructs, Acc. Chem. Res. 38 (2005) 235–242.
[15] K. Suzuki, K. Takao, S. Sato, M. Fujita, Coronene nanophase within coordination spheres: increased solubility of C_{60}, Am. Chem. Soc. 132 (2010) 2544–2545.
[16] A. Mateo-Alonso, D.M. Guldi, F. Paolucci, M. Prato, Fullerenes: multitask components in molecular machinery, Angew. Chem. Int. Ed. 46 (2007) 8120–8126.
[17] F. Diederich, M. Gomez-Lopez, Supramolecular fullerene chemistry, Chem. Soc. Rev. 28 (1999) 263–277.
[18] D.M. Guldi, C. Luo, N.A. Kotov, T. Da Ros, S. Bosi, M. Prato, Zwitterionic acceptor moieties: small reorganization energy and unique stabilization of charge transfer products, J. Phys. Chem. B 107 (2003) 7293–7298.
[19] H. Imahori, K. Hagiwara, M. Aoki, T. Akiyama, S. Taniguchi, T. Okada, M. Shirakawa, Y. Sakata, Linkage and solvent dependence of photoinduced electron transfer in zincporphyrin-C_{60} dyads, J. Am. Chem. Soc. 118 (1996) 11771–11782.
[20] B.M. Illescas, N. Martin, [60]Fullerene-based electron acceptors, C. R. Chim. 9 (2006) 1038–1050.
[21] M.A. Herranz, B. Illescas, N. Martin, C. Luo, D.M. Guldi, Donor/acceptor fulleropyrrolidine triads, J. Org. Chem. 65 (2000) 5728–5738.
[22] B.M. Illescas, N. Martin, [60]Fullerene adducts with improved electron acceptor properties, J. Org. Chem. 65 (2000) 5986–5995.
[23] M. Diekers, A. Hirsch, S. Pyo, J. Rivera, L. Echegoyen, Synthesis and electrochemical properties of new C_{60}-acceptor and-donor dyads, Eur. J. Org. Chem. (1998) 1111–1121.
[24] K. Okamoto, T. Hasobe, N.V. Tkachenko, H. Lemmetyinen, P.V. Kamat, S. Fukuzumi, Drastic difference in lifetimes of the charge-separated state of the formanilide-anthraquinone dyad versus the ferrocene-formanilide-anthraquinone triad and their photoelectrochemical properties of the composite films with fullerene clusters, J. Phys. Chem. A 109 (2005) 4662–4670.
[25] E.M. Perez, A.L. Capodilupo, G. Fernandez, L. Sanchez, P.M. Viruela, R. Viruela, E. Orti, M. Bietti, N. Martin, Weighting non-covalent forces in the molecular recognition of C_{60} relevance of concave–convex complementarity, Chem. Commun. (2008) 4567–4569.
[26] A.A. Bakulin, S.A. Zapunidy, M.S. Pshenichnikov, P.H.M. van Loosdrechta, D.Y. Paraschuk, Efficient two-step photogeneration of long-lived charges in ground-state charge-transfer complexes of conjugated polymer doped with fullerene, Phys. Chem. Chem. Phys. 11 (2009) 7324–7330.
[27] Z.J. Diwu, Novel therapeutic and diagnostic application of hypocrellins and hypericins, Photochem. Photobiol. 61 (1995) 529–539.
[28] G.A. Kraus, W. Zhang, M.J. Fehr, J.W. Petrich, Y. Wannemuehler, S. Carpenter, Research at the interface between chemistry and virology: development of a molecular flashlight, Chem. Rev. 96 (1996) 523–536.
[29] Y. Gao, Z. Ou, J. Chen, G. Yang, X. Wang, B. Zhang, M. Jin, L. Liu, Photodynamic properties of supramolecular assembly constructed by magnesium complex of hypocrellin A and fullerene C_{60}, New J. Chem. 32 (2008) 1555–1560.
[30] Y. Gao, Z. Ou, Z. Zhang, S. Li, G. Yang, X. Wang, Photoinduced electron transfer between perylenequinonoid/fullerene C_{60} supramolecule and electron donor, Acta Phys.: Chim. Sin. 25 (2009) 74–78.
[31] A. Ikeda, Y. Doi, M. Hashizume, J. Kikuchi, T. Konishi, An extremely effective DNA photocleavage utilizing functionalized liposomes with a fullerene-enriched lipid bilayer, J. Am. Chem. Soc. 129 (2007) 4140–4141.
[32] C. Constantin, M. Neagu, R. Ion, M. Gherghiceanu, C. Stavaru, Fullerene–porphyrin nanostructures in photodynamic therapy, Nanomedicine 5 (2010) 307–317.
[33] R. Partha, J.L. Conyers, Biomedical applications of functionalized fullerene-based nanomaterials, Int. J. Nanomed. 4 (2009) 261–275.
[34] K.H. Zhao, L.J. Jiang, Structural modification in hypocrellin pigments, Youji Huaxue 9 (1989) 252–254.
[35] Y. Yamakoshi, T. Yagami, K. Fukuhara, S. Sueyoshi, N. Miyata, Solubilization of fullerenes into water with polyvinylpyrrolidone applicable to biological tests, J. Chem. Soc. Chem. Commun. (1994) 517–518.
[36] J.R. Lakowicz, Principles of Fluorescence Spectroscopy, Kluwer Academic Publishing/Plenum, New York, 1999.
[37] L. Zhang, J. Chen, S. Li, J. Chen, Y. Li, G. Yang, Y. Li, Photophysical and photochemical studies on bis(Dendron) poly(aryl ether) dendrimers: Intramolecular triplet energy transfer in poly(aryl ether) dendrimers via a folded conformation, J. Photochem. Photobiol. A: Chem. 181 (2006) 429–436.
[38] Y. Li, D. Dini, M.J.F. Calvete, M. Hanack, W. Sun, Artificial construction of the magnetically separable nanocatalyst by anchoring pt nanoparticles on functionalized carbon-encapsulated nickel nanoparticles, J. Phys. Chem. A 112 (2008) 472–480.
[39] D. Dubois, K.M. Kadish, S. Flanagan, R.E. Haufler, L.P.F. Chibante, L.J. Wilson, Spectroelectrochemical study of the C_{60} and C_{70} fullerenes and their mono-, di-, tri- and tetraanions, J. Am. Chem. Soc. 113 (1991) 4364–4366.
[40] K.A. Connors, Binding Constants, Wiley, New York, 1987.
[41] J.B. LePecq, C. Paoletti, A fluorescent complex between ethidium bromide and nucleic acids, J. Mol. Biol. 27 (1967) 87–106.
[42] W.A. Pruetz, Inhibition of DNA-ethidium bromide intercalation due to free radical attack upon DNA, Radiat. Environ. Biophys. 23 (1984) 1–6.
[43] I. Renge, Solvent effects on the absorption maxima of fullerenes C_{60} and C_{70}, J. Phys. Chem. 99 (1995) 15955–15962.
[44] Y.P. Sun, C.E. Bunker, Fluorescence of (56)-fullerene-C_{70} in room-temperature solutions: quantum yields and well-resolved spectra as a function of excitation wavelength, J. Phys. Chem. 97 (1993) 6770–6773.
[45] Y. Rio, J. Nierengarten, Water soluble supramolecular cyclotriveratrylene-[60] fullerene complexes with potential for biological applications, Tetrahedron Lett. 43 (2002) 4321–4324.
[46] J.F. Nierengarten, L. Oswald, J.F. Eckert, J.F. Nicoud, N. Armaroli, Complexation of fullerenes with dendritic cyclotriveratrylene derivative, Tetrahedron Lett. 40 (1999) 5681–5684.
[47] M.J. Hardie, C.L. Raston, Confinement and recognition of icosahedral main group cage molecules: fullerene C_{60} and o-, m-, p-dicarbadodecaborane(12), Chem. Commun. (1999) 1153–1163.

[48] I.V. Lijanova, J.F. Maturano, J.G.D. Chavez, K.E.S. Montes, S.H. Ortega, T. Klimova, M. Martinez-Garcia, Synthesis of cyclotriveratrylene dendrimers and their supramolecular complexes with fullerene C_{60}, Supramol. Chem. 21 (2009) 24–34.
[49] Z. Zhou, S. Qian, S. Yao, Z. Zhang, Electron transfer in colloidal TiO_2 semiconductors sensitized by hypocrellin A, Radiat. Phys. Chem. 65 (2002) 241–248.
[50] J. Zhao, T.M. Fyles, T.D. James, Chiral binol-bisboronic acid as fluorescence sensor for sugar acids, Angew. Chem. Int. Ed. 43 (2004) 3461–3464.
[51] A. Hosseini, S. Taylor, G. Accorsi, N. Armaroli, C.A. Reed, P.D.W. Boyd, Calix[4]arene-linked bisporphyrin hosts for fullerenes: binding strength, solvation effects, and porphyrin-fullerene charge transfer bands, J. Am. Chem. Soc. 128 (2006) 15903–15913.
[52] F. D'Souza, R. Chitta, S. Gadde, M.E. Zandler, A.L. McCarty, A.S.D. Sandanayaka, Y. Araki, O. Ito, Potassium ion controlled switching of intra- to intermolecular electron transfer in crown ether appended free-base porphyrin-fullerene donor-acceptor systems, J. Phys. Chem. A 110 (2006) 4338–4347.
[53] M. Yanase, M. Matsuoka, Y. Tatsumi, M. Suzuki, H. Iwamoto, T. Haino, Y. Fukazawa, Thermodynamic study on supramolecular complex formation of fullerene with calix[5]arenes in organic solvents, Tetrahedron Lett. 41 (2000) 493–497.
[54] A. Smirnov, D.B. Fulton, A. Andreotti, J.W. Petrich, Exploring ground-state heterogeneity of hypericin and hypocrellin A and B: Dynamic and 2D ROESY NMR study, J. Am. Chem. Soc. 121 (1999) 7979–7988.
[55] S. Mazzini, L. Merlini, R. Mondelli, L. Scaglioni, Conformation and tautomerism of hypocrellins. Revised structure of shiraiachrome A, J. Chem. Soc., Perkin Trans. 2 (2001) 409–416.
[56] E.M. Perez, M. Sierra, L. Sanchez, M.R. Torres, R. Viruela, P.M. Viruela, E. Orti, N. Martin, Concave tetrathiafulvalene-type donors as supramolecular partners for fullerenes, Angew. Chem. Int. Ed. 46 (2007) 1847–1851.
[57] E.M. Perez, B.M. Illescas, M.A. Herranza, N. Martin, Supramolecular chemistry of p-extended analogues of TTF and carbon nanostructuresw, New J. Chem. 33 (2009) 228–234.
[58] M. Shirakawa, N. Fujita, S. Shinkai, [60]Fullerene-motivated organogel formation in a porphyrin derivative bearing programmed hydrogen-bonding sites, J. Am. Chem. Soc. 125 (2003) 9902–9903.
[59] J. Marois, K. Cantin, A. Desmarais, J. Morin, [3]Rotaxane–porphyrin conjugate as a novel supramolecular host for fullerenes, Org. Lett. 10 (2008) 33–36.
[60] P.V. Kamat, Photoinduced charge transfer between fullerenes (C_{60} and C_{70}) and semiconductor zinc oxide colloids, J. Am. Chem. Soc. 113 (1991) 9705–9707.
[61] M. Weng, M. Zhang, W. Wang, T. Shen, Investigation of triplet states and radical anions produced by laser photoexcitation of hypocrellins, J. Chem. Soc. Faraday Trans. 93 (1997) 3491–3495.
[62] M.E. El-Khouly, M. Fujitsuka, O. Ito, Photoinduced electron transfer between metal octaethylporphyrins and fullerenes (C_{60}/C_{70}) studied by laser flash photolysis: electron-mediating and hole-shifting cycles, Phys. Chem. Chem. Phys. 4 (2002) 3322–3329.
[63] M.E. El-Khouly, Comparative study of the bimolecular electron transfer of fullerenes (C_{60}/C_{70}) and 9 9-disubstituted fluorenes by laser flash photolysis, Photochem. Photobiol. Sci. 6 (2007) 539–544.
[64] Y. Sasaki, Y. Araki, M. Fujitsuka, O. Ito, A. Hirao, H. Nishizawa, Photoinduced electron transfer and electron-mediating systems from aromatic amines to triplet states of C_{60} and C_{70} in the presence of a viologen dication, Photochem. Photobiol. Sci. 2 (2003) 136–141.
[65] C. Jehoulet, A.J. Bard, F. Wudl, Electrochemical reduction and oxidation of C_{60} films, J. Am. Chem. Soc. 113 (1991) 5456–5457.
[66] J.W. Arbogast, C.S. Foote, Photophysical properties of C_{70}, J. Am. Chem. Soc. 113 (1991) 8886–8889.
[67] D.M. Guldi, N. Martin, Fullerene architectures made to order, biomimetic motifs-design and features J, J. Mater. Chem. 12 (2002) 1978–1992.
[68] D.M. Guldi, M. Prato, Excited-state properties of C_{60} fullerene derivatives, Acc. Chem. Res. 33 (2000) 695–703.
[69] Y. He, L. Jiang, Synthesis EPR investigations of new aminated hypocrellin derivatives, Free Radical Biol. Med. 28 (2000) 1642–1650.
[70] K. Yoshizawa, T. Sato, K. Tanaka, T. Yamabe, K. Okahara, ESR study of TDAE-C_{60} and TDAE-C_{70} in solution, Chem. Phys. Lett. 213 (1993) 498–502.
[71] A.S. Lobach, N.F. Goldshleger, M.G. Kaplunov, A.V. Kulikov, Near-IR, ESR studies of the radical anions of C_{60} and C_{70} in the system fullerene-primary amine, Chem. Phys. Lett. 243 (1995) 22–28.
[72] D.R. Lawson, D.L. Feldhiem, C.A. Foss, P.K. Dorhout, C.M. Elliott, C.R. Martin, B. Parkinson, Near-IR absorption spectra for the C_{70} fullerene anions, J. Phys. Chem. 96 (1992) 7175–7177.
[73] M.T. Spiotto, A. Banh, I. Papandreou, H. Cao, M.G. Galvez, G.C. Gurtner, N.C. Denko, Q.T. Le, A.C. Koong, Imaging the unfolded protein response in primary tumors reveals microenvironments with metabolic variations that predict tumor growth, Cancer Res. 70 (2010) 78–88.
[74] M. Seshadri, D.A. Bellnier, L.A. Vaughan, J.A. Spernyak, R. Mazurchuk, T.H. Foster, B.W. Henderson, Light delivery over extended time periods enhances the effectiveness of photodynamic therapy, Clin. Cancer Res. 14 (2008) 2796–2805.
[75] Y. Gao, Z. Ou, G. Yang, L. Liu, M. Jin, X. Wang, B. Zhang, L. Wang, Efficient photocleavage of DNA utilizing water soluble riboflavin/naphthalene substituted fullerene complex, J. Photochem. Photobiol. A: Chem. 203 (2009) 105–111.
[76] Z. Ou, J. Chen, X. Wang, B. Zhang, Y. Cao, Synthesis of a water-soluble cyclodextrin modified hypocrellin and ESR study of its photodynamic therapy properties, New J. Chem. 26 (2002) 1130–1136.
[77] T.T. Williams, C. Dohno, E.D.A. Stemp, J.K. Barton, Effects of the photooxidant on dna-mediated charge transport, J. Am. Chem. Soc. 126 (2004) 8148–8158.
[78] J.M. Lehn, Supramolecular chemistry scope and perspectives molecules, supermolecules, and molecular devices, Angew, Chem. Int. Ed. Engl. 27 (1988) 89–112.
[79] F. D'Souza, P.M. Smith, S. Gadde, A.L. McCarty, M.J. Kullman, M.E. Zandler, M. Itou, Y. Araki, O. Ito, Supramolecular triads formed by axial coordination of fullerene to covalently linked zinc porphyrin-ferrocene(s): design, syntheses, electrochemistry, and photochemistry, J. Phys. Chem. B 108 (2004) 11333–11343.